Real–Time Speciation of Uranium during Active Bioremediation and U(IV) Reoxidation

John Komlos[1]; Bhoopesh Mishra[2]; Antonio Lanzirotti[3]; Satish C. B. Myneni[4]; and Peter R. Jaffé[5]

Abstract: The biological reduction of uranium from soluble U(VI) to insoluble U(IV) has shown potential to prevent uranium migration in groundwater. To gain insight into the extent of uranium reduction that can occur during biostimulation and to what degree U(IV) reoxidation will occur under field relevant conditions after biostimulation is terminated, X-ray absorption near edge structure (XANES) spectroscopy was used to monitor: (1) uranium speciation in situ in a flowing column while active reduction was occurring; and (2) in situ postbiostimulation uranium stability and speciation when exposed to incoming oxic water. Results show that after 70 days of bioreduction in a high (30 mM) bicarbonate solution, the majority (>90%) of the uranium in the column was immobilized as U(IV). After acetate addition was terminated and oxic water entered the column, in situ real-time XANES analysis showed that U(IV) reoxidation to U(VI) (and subsequent remobilization) occurred rapidly (on the order of minutes) within the reach of the oxygen front and the spatial and temporal XANES spectra captured during reoxidation allowed for real-time uranium reoxidation rates to be calculated.

DOI: 10.1061/(ASCE)0733-9372(2008)134:2(78)

CE Database subject headings: Uranium; Biodegradation; Oxidation; Iron; Rates.

Introduction

Uranium contamination is a concern at numerous U.S. Department of Energy facilities throughout the United States. Uranium exists in nature as either U(VI) or U(IV). The oxidized form, U(VI), tends to be soluble and may exist as different ions depending on the alkalinity and pH [e.g. UO_2^{2+}, $UO_2\ (CO_3)_2^{2-}$]. It typically transports in flowing groundwater, whereas the reduced form of uranium, U(IV), forms insoluble minerals such as UO_2 (uraninite) that precipitates out of solution. The bioreduction of U(VI) to U(IV) is an anaerobic process that has been shown to occur after nitrate is consumed (Finneran et al. 2002; Senko et al. 2002) and during either iron and/or sulfate reducing conditions (Abdelouas et al. 1999; Anderson et al. 2003; Lovley and Phillips 1992). The precipitation of uranium from groundwater through the addition of an electron donor to stimulate the uranium reducing microbial population has shown potential to prevent uranium migration from contaminated sites (Anderson et al. 2003; Chang et al. 2005; Istok et al. 2004).

The nature of U(VI) reduction, however, in anoxic sediments is poorly understood. Some studies have shown that the majority of uranium in sediments under biologically reducing conditions was present as U(IV) (Michalsen et al. 2006; Sani et al. 2005), although other studies have shown that not all of the uranium measured on mineral surfaces under reducing conditions was reduced (Gu et al. 2005a; Jeon et al. 2004; Ortiz-Bernad et al. 2004; Wan et al. 2005) and the reasons for the presence of U(VI) under reducing conditions are inconclusive. Possible explanations are that U(VI) was adsorbed and unavailable for microbial reduction. U(VI) can adsorb to Fe(III)–(hydr)oxides (Giammar and Hering 2001; Jeon et al. 2004) or form relatively insoluble complexes with PO_4^{3-} (Cheng et al. 2006; Langmuir 1978), and research have shown that U(VI) sorption can limit the rate and extent of microbial U(VI) reduction (Jeon et al. 2004). Calcium can suppress U(VI) sorption (Zheng et al. 2003) but has been shown to also strongly inhibit U(VI) reduction (Brooks et al. 2003) and to increase abiotic ferrihydrite-dependent U(IV) oxidation (Ginder-Vogel et al. 2006). In carbonate containing groundwater at circumneutral pH, U(VI) forms strong soluble complexes with CO_3^{2-} (e.g., UO_2CO_3, $UO_2(CO_3)_2^{2-}$, $UO_2(CO_3)_3^{4-}$) (Fredrickson et al. 2000) that absorb poorly with mineral surfaces such as Fe(III) (hydr)oxides (Duff and Amrhein 1996; Hsi and Langmuir 1985) and clays due to the neutral or anionic charge (Fredrickson et al. 2000). In (bi)carbonate containing waters under reducing conditions, the majority of the uranium has been shown to be U(IV) (Sani et al. 2005; Wan et al. 2005) or as a combination of U(VI) and U(IV) (Gu et al. 2005a; Wan et al. 2005) and the reasons for the discrepancy are not fully understood. The U(VI) complexes mentioned above could decrease U(VI) bioavailability in the (bi)carbonate solution. In addition, U(IV) can be anaerobically oxidized by denitrification byproducts (Senko et al. 2002) and, under electron donor limitation, U(IV) can be oxidized by Fe(III) (Ginder-Vogel et al. 2006; Sani et al. 2005) and Mn–

[1]Research Staff, Dept. of Civil and Environmental Engineering, Princeton Univ., Princeton, NJ 08544. E-mail: jkomlos@princeton.edu

[2]Research Associate, Dept. of Geosciences, Princeton Univ., Princeton, NJ 08544. E-mail: bmishra@Princeton.edu

[3]Senior Research Associate, The Univ. of Chicago—Center for Advanced Radiation Sources at the National Synchrotron Light Source, Brookhaven National Laboratory, Upton, NY 11973. E-mail: lanzirotti@bnl.gov

[4]Associate Professor, Dept. of Geosciences, Princeton Univ., Princeton, NJ 08544. E-mail: smyneni@Princeton.edu

[5]Professor, Dept. of Civil and Environmental Engineering, Princeton Univ., Princeton, NJ 08544 (corresponding author). E-mail: jaffe@princeton.edu

Note. Discussion open until July 1, 2008. Separate discussions must be submitted for individual papers. To extend the closing date by one month, a written request must be filed with the ASCE Managing Editor. The manuscript for this paper was submitted for review and possible publication on April 11, 2007; approved on August 3, 2007. This paper is part of the ***Journal of Environmental Engineering***, Vol. 134, No. 2, February 1, 2008. ©ASCE, ISSN 0733-9372/2008/2-78–86/$25.00.

oxides (Fredrickson et al. 2002). Increased bicarbonate concentrations from microbial respiration has been shown to increase the favorability of Fe(III)-dependent U(IV) oxidation to U(VI) (Ginder-Vogel et al. 2006; Wan et al. 2005). However, others have shown that little bioreduced U(IV) was reoxidized under anaerobic conditions even in bicarbonate concentrations as high as 1 M (Elias et al. 2003; Zhou and Gu 2005).

The above paragraph demonstrates that a variety of factors govern the rate and extent of U(VI) bioreduction and biogenic U(IV) stability. Additional research is necessary to better understand the nature of uranium under reducing conditions to successfully predict uranium stability during biostimulation. It is also important to understand U(IV) stability when biostimulation is stopped and oxic conditions are reintroduced either through groundwater transport or infiltration of oxygenated rainwater. U(IV) has been shown to oxidize very fast in the presence of oxygen (Gu et al. 2005b; Zhou and Gu 2005) which could potentially negate any uranium immobilization during biostimulation. However, Gu et al. (2005b) and Zhou and Gu (2005) only dealt with uranium reoxidation in completely mixed (batch) environments. Research is lacking regarding U(IV) reoxidation under more field relevant (flowing) conditions and the effect of oxidant transport through porous media on the spatial and temporal reoxidation of U(IV) is not fully understood. It has been shown that very little oxygen breakthrough occurred compared to the breakthrough of another oxidant (nitrate) during the reoxidation of columns that previously experienced reducing conditions, indicating that oxygen reacts more strongly with other reduced species in addition to uranium (Moon et al. 2007). It was postulated that oxygen is consumed as a sharp front moving through porous media but it is unclear if this is true. How an oxidant moves through a previously reduced zone is important to understand and predict the long term stability of U(IV). Therefore, in addition to understanding uranium speciation during bioremediation, it is also necessary to examine biogenic U(IV) oxidation under field relevant conditions to understand the rate and extent of U(IV) oxidation that could occur after field-scale uranium bioremediation efforts have terminated.

The goal of the research presented herein was to examine uranium speciation in situ (while a flowing column was operating under reducing conditions) using X-ray absorption near edge structure (XANES) spectroscopy to determine the species of uranium present under active biological reducing conditions (i.e., continuous electron donor addition) without the possibility of oxygen contamination. The reduced sediment was then reoxidized with dissolved oxygen while XANES spectroscopy measured in situ how fast and to what extent uranium reoxidizion occurs under field-relevant (flow-through) conditions. To the writers' knowledge, the research presented herein is the first to measure uranium speciation in a flowing column in situ under actively reducing conditions as well as during U(IV) reoxidation.

Material and Methods

Sediment Description

The sediment used was obtained from a former uranium processing site at Old Rifle, Colo., which is a Uranium Mill Tailings Remedial Action (UMTRA) site, part of the U.S. Department of Energy's (DOE's) Environmental Remediation Sciences Program. A description of the site as well as groundwater characteristics can be found in Anderson et al. (2003). The sediment was designated Rifle area background sediment (RABS). The previously saturated sediment was dried, sieved (<2 mm), and stored at 4 °C until use. Chemical characteristics of the RABS sediment (e.g., organic, Fe, U content) can be found in Moon et al. (2007).

Column Design and Operation

The column used in this experiment was fabricated from acrylic tubing (15 cm long, 5.08 cm i.d., 0.64 cm wall thickness) with Delrin end caps (both from McMaster Carr). The end caps were fitted with a 0.64-cm-thick filter made of ultrahigh molecular weight hydrophobic polyethylene porous plastic with a 20 μm pore size (GenPore, Reading, Pa.). The column wall was machined down to 1.0 mm for the 15 cm length of the soil sample, providing a flat rectangular profile (2.5 cm × 15 cm) that allowed for a perpendicular alignment with the incoming X-rays for the XANES measurements described below [based on the design by Wan et al. (2005)]. The column was wet packed with 540 g of sediment and 97 mL of deionized water resulting in an initial porosity of 0.33.

Prior to bioreduction, the columns were first flushed with 30 mM sodium bicarbonate until no uranium was detected in the effluent. A simulated groundwater solution containing 20 μM uranyl acetate, 30 mM sodium bicarbonate, 0.14 mM NH_4Cl, 0.014 mM $NaH_2PO_4 * H_2O$, 0.045 mM KCl, 0.33 mL/L of a trace vitamins solution (Lovley and Phillips 1988), and 0.33 mL/L of a trace minerals solution (Lovley and Phillips 1988) was then pumped up-flow through the column at a rate of 0.2 mL/min 14 days prior to the commencement of electron donor (3 mM acetate) addition to allow the uranium to break through the column and equilibrate before electron donor addition (i.e., biostimulation) commenced. The influent media was continuously purged with CO_2/N_2 gas (20:80) which, combined with 30 mM bicarbonate, maintained the pH at 7 throughout the experiment. The relatively high bicarbonate concentration reproduced a biostimulation scenario where elevated bicarbonate concentrations would be expected due to enhanced microbial activity (Wan et al. 2005). Sulfate (present in the trace mineral solution) and phosphate concentrations were kept relatively low (9 and 14 μM, respectively) to minimize the influence of sulfate reduction and the formation of uranyl–phosphate complexes.

Just before electron donor addition commenced, 1 pore volume of *Geobacter metallireducens* was added to the column and flow was shut off for 12 h. The growth culture was prepared by growing *G. metallireducens* on acetate and ferric citrate for 5 days in a bicarbonate buffered growth media prepared as previously described (Komlos and Jaffe 2004). After 5 days, the growth culture was rinsed to remove aqueous Fe (II) by centrifuging ($5{,}900 \times g$) for 20 min, anaerobically removing the supernatant and replacing with influent media purged with CO_2/N_2 gas (20:80). *G. metallireducens* was chosen because of its ability to reduce U(VI) and Fe(III) with acetate as the electron donor and because it has been shown to be a dominant organism during biostimulation near the area where the sediment was collected (Chang et al. 2005).

Reducing conditions were initiated by stimulating the microbial community via 3 mM sodium acetate addition using a syringe pump (KD Scientific) just upstream of the column influent. On the 64th day of bioreduction the column was taken offline and the inflow and outflow tubes were clamped shut to avoid fluid leakage and exposure to air. The column was packed on ice and shipped overnight to the National Synchrotron Light Source (NSLS) at Brookhaven National Laboratory. The column was

J. Environ. Eng., 2008, 134(2): 78-86

then restarted on Day 65 at the NSLS facility and operated under the same biostimulation conditions described above for 4 days to allow for the system to come back to pretransfer conditions in case some changes occurred during transportation. XANES spectroscopic analysis was performed at Beamline X26A on Day 69 while the column was maintained under flowing conditions.

In order to mimic the cessation of electron donor addition after biostimulation in the field, the column reoxidation was initiated on Day 70 by stopping the electron donor addition and substituting the CO_2/N_2 (20:80) gas supplied to the influent media with a gas containing $O_2/CO_2/N_2$ (20:20:60). The influent media was the same used for bioreduction minus NH_4Cl and the vitamin solution (to prevent dissolved oxygen consumption from ammonia oxidation). CO_2 (20%) and bicarbonate (30 mM) addition was continued during reoxidation to maintain a pH of 7. The column remained at NSLS during reoxidation and was also analyzed on Days 71 and 99. The column was operated at 22–25°C until it was shipped on ice overnight back to Princeton University where it was destructively sampled in an anaerobic glove box (3:97 $H_2:N_2$).

Ex Situ XANES Sample Preparation

Sediment used for the ex situ XANES spectroscopy analysis was from a column bioreduced under the same conditions as described above except for undergoing reducing conditions for an additional 34 days (and no reoxidation). The column was taken apart and the sediment removed from the column using a long spatula in an anaerobic glove box (3:97 $H_2:N_2$), placed in a polycarbonate sample holder and sealed on both sides with two layers of Kapton tape. The samples were placed in a pressurized chamber filled with N_2 gas and transported to Brookhaven National Laboratory for XANES analysis. The XANES spectra of these samples were collected in air.

Batch Uranium Reduction Experiment

One g of RABS sediment and 9.3 mL of the influent media described above (except that the uranyl acetate concentration was 1 mM) was added to 15 mL plastic centrifuge tubes and purged for 30 min with a 20% CO_2/80% N_2 gas mixture prior to being capped with a thick rubber stopper. At the start of the experiment, U(VI) bioreduction was facilitated by the addition of 0.2 mL of 1 M sodium acetate (resulting in 20 mM acetate after mixing) and 0.5 mL of *G. metallireducens* growth culture (prepared and rinsed as described above). The samples were stored in the dark at 22–23°C until analyzed after 35 days using extended X-ray absorption fine structure (EXAFS) spectroscopy as described below. Plastic centrifuge tubes were used to allow for EXAFS analysis of the sediment in situ through the plastic.

Analytical Measurements

Effluent Fe(II) concentrations were measured by adding 0.5 mL of effluent solution to 0.5 mL of 1 M HCl and analyzing after 1 h extraction using ferrozine (Lovley and Phillips 1987). Dissolved oxygen was measured using a Corning 317 dissolved oxygen (DO) meter fitted to an in-line sampling device attached to the effluent of the column. Anions (bromide, acetate, sulfate, phosphate) were analyzed using a Dionex DX500 ion chromatograph equipped with a CD25 conductivity detector and a Dionex IonPac AS14-4 mm column. Influent and effluent U(VI) concentrations were analyzed using reversed phased chromatography coupled to postcolumn derivatization with the dye Arsenazo III (Sigma-Aldrich) as described by Lack et al. (2002). All samples were filtered (0.2 μm) and stored at 4°C until analyzed. The total uranium concentration [U(VI) plus U(IV)] in the sediment was quantified by adding 2–3 g of sediment to 5 mL of 0.2 M $NaHCO_3$. The samples were extracted under aerobic conditions to oxidize U(IV) to U(VI) for 24 h, filtered (0.2 μm), and stored at 4°C until U(VI) was analyzed as described above.

XANES Spectroscopy Measurements

XANES spectroscopy was used to provide information about the oxidation state of uranium. Uranium L_3 edge (17,166 eV) XANES spectroscopy measurements were performed at X26A at the NSLS (Brookhaven National Laboratory). X26A is a hard X-ray microprobe bending magnet (BM) beamline. The energy of the incident X-rays was scanned by using a Si(111) reflection plane of a channel-cut monochromator cooled to 11°C using a Neslab chiller. The X-ray spot size used for these measurements was set to 5×5 μm. The fluorescence signal of the soil column was measured using a Canberra 9-element Ge array detector. The scans were aligned by collecting uranyl acetate solution data after every 3–4 XANES scans. Scan to scan variation in the energy calibration of the monochromator was within 0.2 eV even after several hours. However, a bigger difference was usually seen after each beam refill or beam dump.

Step scans (energy scans with 0.5 eV step size, near the edge and 5.0 eV far below and above the edge) were used with an integration time of 5–15 s per point depending on the signal to noise ratio of the spectra. The bioreduced samples were scanned from −200 to +300 eV relative to edge position to ensure proper normalization and background removal of the data. However, a faster scanning setup was required to monitor the in situ reoxidation profile of the column. Hence the data collected for 0–2 h reoxidation was scanned from −50 to +150 eV relative to the edge position (resulting in a scan time of ~20 min). This energy range was sufficient for linear combination fitting (LCF) of XANES data. All XANES data reported in this study were normalized and fit in this data range for consistency.

XANES Spectroscopy Data Processing and Fitting

Interactive data language (IDL) software associated with Beamline X26A was used to collect data. The data were analyzed using ATHENA (Ravel and Newville 2005) which is based on AUTOBK (Newville et al. 1993) to remove the background. ATHENA was also used for LCF of the uranium data to quantify the relative amount of U(IV) compared to U(VI) in a given spectra. The fitting was done in the normalized $\mu(E)$ space. A fitting range of −50–+150 eV was used for proper normalization of the XANES spectra. Since uranium is known to be stable in +IV and +VI oxidation states only, powdered UO_2 and UO_3 XANES spectra were used as U(IV) and U(VI) standards for the LCF of the sediment samples. The sum of their contribution in the unknown samples was forced to sum to 1. A lower R factor and χ^2_v values were used as the criteria for the goodness of fit. The accuracy of the valance state determination of uranium from the XANES data was estimated to be 10–15%, which is similar to the accuracies previously reported for this analysis (Boyanov et al. 2007; Jeon et al. 2004). Hence 90 and 100% bioreduction should be considered roughly the same for the treatment presented in this study.

J. Environ. Eng., 2008, 134(2): 78-86

EXAFS Measurements

EXAFS spectroscopy was used to provide information about the type, number, and radial distances of the atoms surrounding uranium. Uranium L_3 edge (17,166 eV) EXAFS spectroscopy measurements were performed at X18B at the NSLS (Brookhaven National Laboratory). A channel cut Si(111) crystal was used as a monochromator. The higher harmonics were rejected by detuning the monochromator crystal by 30%. The incident ionization chamber was filled with 100% N_2 gas. The transmitted and reference ion chambers were filled with 100% Ar gas. The fluorescence detector in the Stern–Heald geometry (Stern and Heald 1983) was filled with Ar gas. Uranyl acetate solution was used as a reference and to calibrate energy.

EXAFS Spectroscopy Data Processing and Fitting

The data were analyzed using the methods described within the UWXAFS package (Stern et al. 1995). The background removal procedure is based on the AUTOBK method (Newville et al. 1993) and implemented by using the ATHENA (Ravel and Newville 2005) interface to IFEFFIT (Newville 2001). The theoretical model of uraninite (UO_2) was optimized to the measured spectra using the program FEFFIT (Newville et al. 1995). The theoretical model was built by using FEFF8 (Ankudinov et al. 1998). The data sets were aligned and the backgrounds were removed using the ATHENA program. The input parameter to ATHENA that determines the maximum frequency of the background, R_{bkg}, was set to 1.1 Å (Newville et al. 1993). The data range used for Fourier transforming the EXAFS $\chi(k)$ data was 2.3–10.2 $Å^{-1}$ with a Hanning window function and a delta k value of 1.0 $Å^{-1}$ (Newville et al. 1993). Simultaneous fitting with multiple k weighting (k^1,k^2,k^3) was performed using the Fourier transformed $\chi(R)$ spectra. The fitting range was 1.2–4.4 Å. The simultaneous fitting approach reduces the possibility of obtaining erroneous parameters due to correlations at any single k weighting (Kelly et al. 2002).

XRF Mapping

X-ray fluorescence (XRF) mapping was used to provide element specific information about the spatial distribution of the atoms surrounding uranium. A Canberra nine-element Ge array detector was used for uranium XRF mapping at microscale using a 5×5 μm beam. The incident energy of the X-ray was 17,200 eV and a step size of 35 μm was used with 3 s pixel counting time. Sediment samples were packed into a polycarbonate sample holder and sealed with Kapton tape prior to transport to Beamline X26A at the NSLS at Brookhaven National Laboratory.

Results and Discussion

Abiotic Uranium Transport

A U(VI) and conservative tracer (bromide) breakthrough curve performed prior to the start of biostimulation (Fig. 1) showed that the pore-water and U(VI) residence times in the column were 7.5 and 23.5 h, respectively, resulting in a uranium retardation factor (R) of 3.1. The measured pore-water residence time is faster than the theoretical residence time (8.1 h) indicating that some channeling did occur in the column. A partitioning coefficient (K_d) was calculated using Eq. (1), where the porosity (n) and the bulk

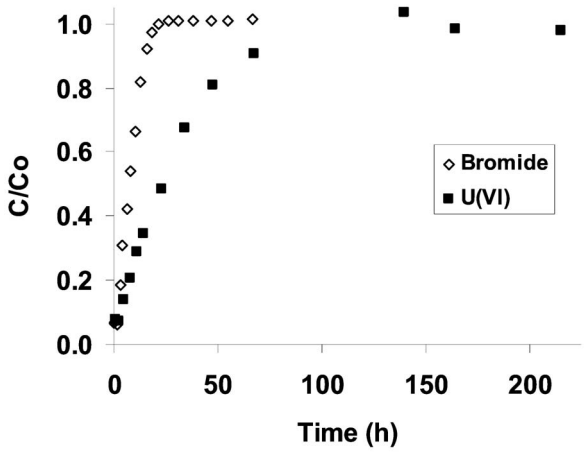

Fig. 1. Bromide (open symbol) and U(VI) (closed symbol) breakthrough prior to biostimulation

mass density (ρ_b) were estimated to be 0.33 and 1.8 g/cm^3, respectively, from the initial conditions of the column (Freeze and Cherry 1979)

$$K_d = (R-1)\frac{n}{\rho_b} \quad (1)$$

The resulting K_d value of 0.38 mL/g corresponded to a previously measured batch K_d value of 0.36 mL/g using the same sediment and media (Moon et al. 2007). Comparison of the U(VI) mass lost to that of the conservative tracer concluded that 6.9 μmoles U(VI) were sorbed onto the media prior to U(VI) breakthrough. After uranium breakthrough, the uranium concentrations in the column influent and effluent were identical (no abiotic loss of uranium) (Fig. 2).

Uranium Bioreduction

The addition of *G. metallireducens* and 3 mM acetate (starting at $t=0$) resulted in the detection of U(VI) removal within 3 days (Fig. 2) with the magnitude of U(VI) removal increasing over time. During the bioreduction period, a cumulative amount of

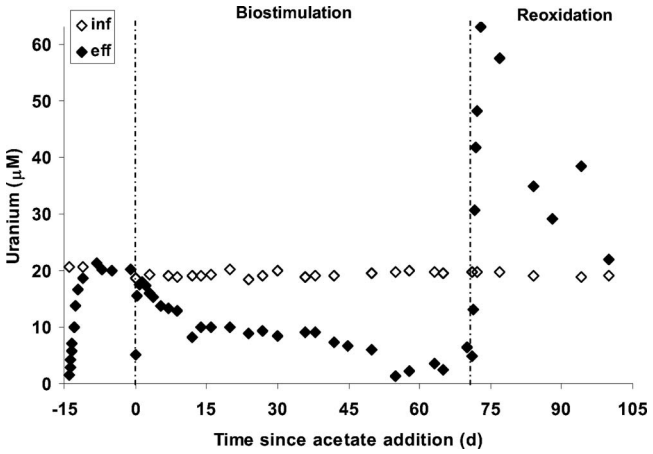

Fig. 2. Influent (open symbol) and effluent (closed symbol) uranium concentrations before bioreduction (–15–0 days), during bioreduction (0–70 days) and during reoxidation (71–99 days)

J. Environ. Eng., 2008, 134(2): 78-86

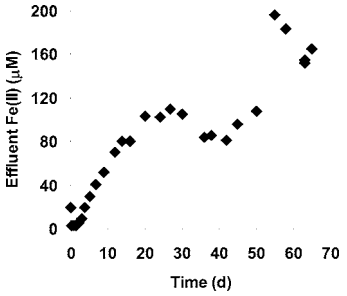

Fig. 3. Effluent Fe(II) concentrations during bioreduction

231 μmoles of U(VI) was removed between the influent and effluent of the column. The effluent pH remained constant at 7.0 during biostimulation. Fe(III) reduction [and subsequent Fe(II) production, Fig. 3] occurred simultaneously with U(VI) reduction (Fig. 2) although neither process reached steady-state conditions by the start of reoxidation on Day 70, indicating that the overall biological activity was still increasing. The effluent Fe (II) concentration was 165 μM after 70 days of biostimulation. Removal of sulfate between the influent and effluent of the column was first detected on Day 16 with 70–96% of the influent 9 μM concentration removed between Day 26 and the end of biostimulation (data not shown). Effluent acetate concentrations remained above 1 mM throughout biostimulation (acetate was not limiting). Phosphate (14 μM) present in the influent media was not detected at the column effluent prior to acetate addition and remained below detection at the effluent throughout biostimulation (data not shown). The lack of phosphate at the effluent is in contrast to U(VI), whose effluent concentration equaled the influent concentration prior to biostimulation and slowly decreased with time of biostimulation (Fig. 2). The discrepancy between the trends of phosphate and U(VI) removal indicates that the U(VI) removal in these experiments was not dependent on complexation with phosphate which corresponds to previous work (Sandino and Bruno 1992) showing that U(VI) will be associated with aqueous phosphate complexes when the $[PO_4^{3-}]_T/[CO_3^{2-}]_T$ ratio is greater than 10^{-1} (which is higher than the ratio in this study, 0.0004). In addition, the calcium concentration in the feed media (0.023 mM) was lower than that observed to inhibit U(VI) reduction (Brooks et al. 2003). Therefore, for these conditions, phosphate and calcium complexes did not appear to play a role in U(VI) reduction.

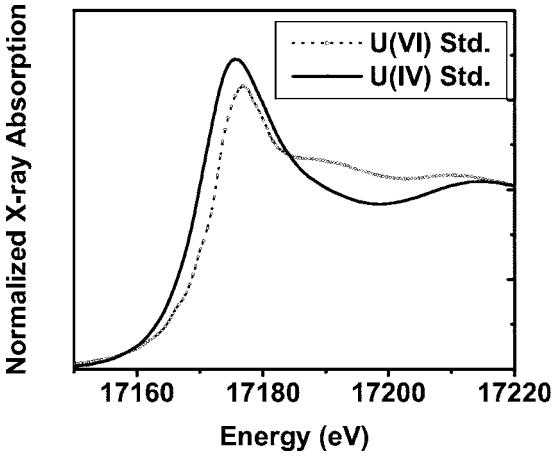

Fig. 4. XANES spectrum of U(VI) and U(IV) standard

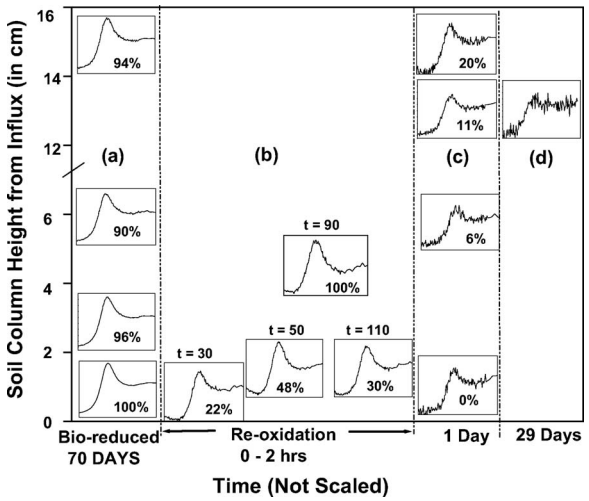

Fig. 5. XANES spectrum showing U speciation: (a) after 70 days of bioreduction; (b) during first 2 h of reoxidation; (c) 1 day after reoxidation; and (d) 29 days after reoxidation. Relative ratio of U(IV) to total uranium is shown (in percentage) in each XANES spectra. Also time (t) is indicated in min for the first 2 h of reoxidation.

Uranium Speciation during Bioreduction

Fig. 4 compares uranium XANES data from UO_2 and UO_3 standards. A higher energy position of the absorption edge and a shoulder at 17,190 eV indicate uranium in the +VI valance state and uranyl coordination geometry. A lower energy position of the edge, a lack of the shoulder at 17,190 eV, and higher amplitude of the peak immediately after the edge indicate uranium in the +IV valance state (Boyanov et al. 2007; Ilton et al. 2006; Michalsen et al. 2006; O'Loughlin et al. 2003; Wan et al. 2005; Wu et al. 2006).

Fig. 5(a) shows XANES spectra of the uranium sediment at different heights of the column after 70 days of bioreduction. LCF indicated that the majority (> 90%) of the uranium was found as U(IV). Further, X-ray fluorescence mapping of the sediment samples from a column experiment using the same sediment under identical experimental conditions (though bioreduced for slightly longer, 104 days) indicated that uranium was homoge-

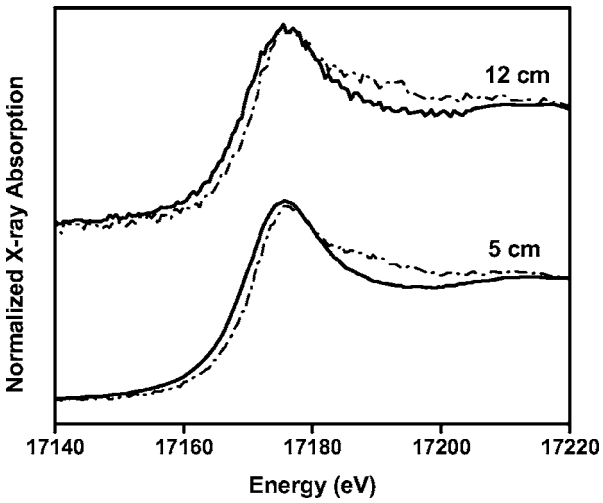

Fig. 6. XANES spectra of in situ (solid line) and ex situ (dash line) measurements at 5 and 12 cm from influx into column

J. Environ. Eng., 2008, 134(2): 78-86

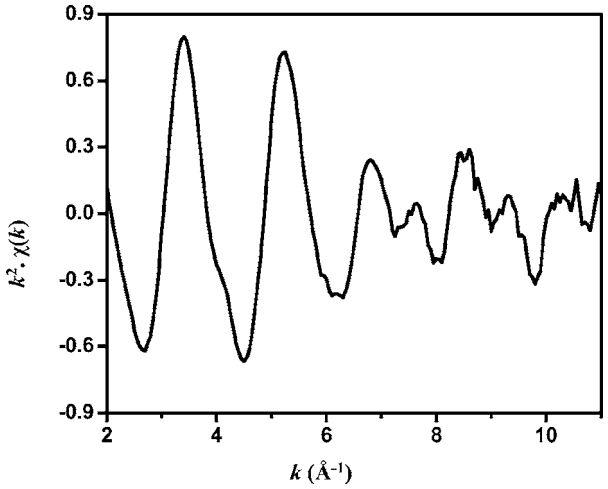

Fig. 7. k^2 weighed $\chi(k)$ data for bioreduced uranium sediment. Data range used for Fourier transform was 2.3–10.2k (Å^{-1}).

neously distributed throughout the sediment (data not shown). The lack of uranium hotspots in the sediment indicates that the measured XANES spectra are representative of the sediment and do not represent any localized feature. Complete reduction of U(VI) to U(IV) under bioreduced conditions contradicted XANES spectroscopy performed on ex situ sediment samples from the 104 day bioreduction column mentioned above where not all of the uranium was reduced (Fig. 6). The discrepancy between the ex situ and in situ XANES analysis was unexpected and could have been caused by oxygen contamination during sample preparation, transport, or analysis (even though efforts were taken to provide anaerobic conditions). The discrepancy could also have been due to electron donor limitation once acetate addition was terminated and the sample was removed from the column, thus allowing U(IV) to act as an electron donor for Fe (III) reduction. Ferrihydrite has been shown to oxidize U(IV) under conditions with electron donor limitation (Ginder-Vogel et al. 2006) and additional research is needed to determine the impact of available Fe (III) in the RABS sediment on U(IV) stability under electron donor limiting conditions.

Table 1. EXAFS Fitting Parameters

Path	Coordination number (N)	Bond length (R) (Å)	Debye–Waller factor (σ^2) (10^{-3} Å^2)
U-O1	7.5±0.6	2.34±0.01	12.2±1.5
U-U1	5.3±1.4	3.84±0.01	8.6±2.8
U-MS	7.5±0.6	4.68±0.02	24.4±3.0

Note: MS denotes two multiple scattering paths: U-O1-U-O1. Passive electron reduction factor (S_0^2) was set at 0.9, and ΔE was 3.1±0.6. Fourier transform was done over the data range of 2.3–10.2Å^{-1}, and the fit range was 1.2–4.4 Å.

EXAFS analysis of a sample run in a batch experiment with similar experimental conditions as the bioreduced column sediment was performed to further investigate the speciation of the uranium in the column under active bioreduction conditions. The EXAFS data quality can be seen from the averaged EXAFS $\chi(k)*k^2$ spectrum in Fig. 7. Fig. 8 shows the $\chi(k)*k^2$ magnitude and real part of the Fourier transform and fit of the bioreduced uranium sediment sample. The peak at 1.8 Å is due to the cubical oxygen shell in UO_2, and the double peak between 2.5 and 4.5 Å is mostly due to the 12-member U shell at 3.87 Å in UO_2. The 1:1 ratio of the peak amplitudes between 2.5 and 4.5 Å is consistent with previously published results for uranium nanoparticulates (O'Loughlin et al. 2003) which is different from the 1:2 ratio found for a pure UO_2 standard (Boyanov et al. 2007; O'Loughlin et al. 2003). EXAFS modeling of this sample was done using the model for UO_2 crystal structure (O'Loughlin et al. 2003). Best fit values for the EXAFS analysis are listed in Table 1. The best fit value for the number of first shell oxygen atoms is 7.5±0.6 at 2.34 Å, which is consistent with the UO_2 structure of eight oxygen atoms in the first shell at the same distance. The drop in average U–U coordination from 12 in crystalline UO_2 to 5.3±1.4 in the bioreduced sediment could be either due to a thin coating of UO_2 on Fe particles present in the sediment or the formation of the nanometer sized uraninite particles, both of which indicate the formation of uraninite nanophases.

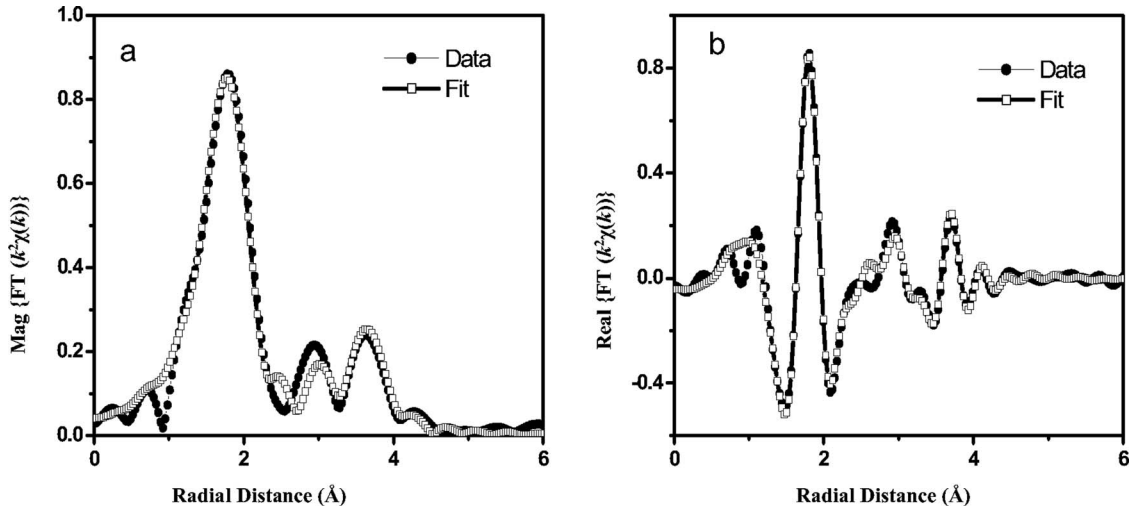

Fig. 8. Magnitude (a); real part (b) of Fourier transform of $\chi(k)*k^2$ best-fit model and data from bioreduced sediment

J. Environ. Eng., 2008, 134(2): 78-86

Table 2. U(IV) Reoxidation Kinetics throughout Column

Reoxidation time	Distance into column	U(IV) reoxidized (%)	Reoxidation rate (μmol/g/h)[a]
0–30 min	0.5 mm	78	0.667
50–110 min	2.0 cm	15	0.077
0–24 h	6.0 cm	84	0.015
0–22.5 h	15.0 cm	74	0.014

[a]The U(IV) concentration just before reoxidation (0.43 μmol/g) was estimated from the mass of U(VI) precipitated during biostimulation (231 μmol, Fig. 2), mass of sediment in the column (540 g), and the assumption that the uranium was uniformly precipitated throughout the column.

Reoxidation of Bioreduced Uranium

The switchover of column inflow containing deoxygenated water and acetate to oxic water without acetate resulted in the rapid resolubilization and removal of uranium from the column (Fig. 2). XANES spectroscopic analysis conducted on the column during reoxidation monitored the spatial and temporal transformation of U(IV) to U(VI) over time [Figs. 5(b–d)]. U(IV) reoxidation at the beginning of the column (0.5–2 cm) was detected within 30 min of DO addition, with significant (70%) reoxidation occurring at 2 cm by 2 h. However, no U(IV) oxidation was observed 5 cm into the column after 1.5 h of the switchover. A conservative (bromide) tracer breakthrough curve performed at the start of reoxidation measured the hydraulic detention time during reoxidation to be 3.0 h (resulting in a linear velocity of 5 cm/h). The decrease in time of bromide breakthrough from the start of biostimulation (7.5 h) to the start of oxidation (3.0 h), which indicates an increase in channeling, was caused by transport of the column by courier from the laboratory to NSLS for analysis. If the DO had not reacted with any reduced species, it should have transported 7.5 cm into the column after 1.5 h. Therefore, the lack of oxidation at 5 cm after 1.5 h and the oxidation of uranium at the beginning of the column [Fig. 5(b)] indicates that DO was retarded through reaction with U(IV) and other reduced species. In addition, significant (>50%) reoxidation of U(IV) at 2 cm but no measurable U(IV) oxidation at 5 cm after 1.5 h indicates that the uranium was being oxidized as a sharp front through the column. XANES spectroscopic analysis after 1 day [Fig. 5(c)] shows that U(IV) was oxidized throughout the column (though to a lesser degree further into the column). The deterioration of the XANES signal from the beginning of reoxidation to days 1 and 29 of reoxidation [where the XANES spectra were too noisy for effective quantitative distinction between U(IV) and U(VI)] indicates that the total mass of U was being removed from the sediment and leaving the system (Fig. 5). Slight variations were observed during reoxidation between XANES spectra at different locations in the column that had similar U(IV)/U(VI) ratios. This suggests different types of U(VI) complexation may have occurred at different spots in the column and warrants future investigation of the detailed local coordination environment using EXAFS analysis.

The spectra from Fig. 5 was used to calculate the U(IV) reoxidation rate at different distances along the length of the column and different times of reoxidation (Table 2). The U(IV) reoxidation rate at the beginning of the column within the first 0.5 h was 0.67 μmol/g/h and decreased over time and distance into the column. The reoxidation rate at the beginning of the column (78% within 30 min) was faster than reported for oxygen dependent U(IV) oxidation in a batch experiment with 1 M bicarbonate (~1 h half-life) (Zhou and Gu 2005) and a field push-pull test with 30 mM bicarbonate (~40 min half-life) (Gu et al. 2005b). The decrease in uranium reoxidation rate with distance into the column and time of reoxidation was likely influenced by oxygen depletion with distance into the column. It is important to note, however, that U(IV) reoxidation rates are an underestimate of the actual reoxidation rates due to loss of uranium mass as a result of remobilization from the sediment. This is evident from the decrease in XANES intensity (visualized from the increase in the noise of the XANES spectra) after 1 day of reoxidation (Fig. 5). A qualitative assessment of the loss of signal intensity after 2 h, 1 day, and 29 days of reoxidation was ~50, ~80, and ~90%, respectively.

Due to logistical constraints, DO was not measured continuously throughout reoxidation but was measured at the effluent after 29 days of reoxidation to be 0.7 mg/L (8.3% of influent media). This indicates that although some DO broke through the column, the majority was still consumed in the column at that time. A comparison of the uranium precipitated over time during the bioreduction phase (229 μmoles) to the amount of uranium resolubilized after 29 days of reoxidation (165 μmoles) (Fig. 2) showed that 76% of the precipitated uranium was removed during 29 days of reoxidation, and that 64 μmoles uranium remained in the column. This corresponds well to the mass of uranium in the column determined via extraction at the termination of the experiment. The average surface associated uranium concentration determined via extraction was 0.08 ($\pm 0.05, n=6$) μmol/g, corresponding to a total mass of uranium remaining in the column of 46 μmoles.

Implications regarding Uranium Transport in Sediments

These results show that during active bioreduction most of the uranium in the column was in the form of U(IV) [and not as sorbed U(VI)] when uranyl–phosphate and uranyl–calcium complexes were minimized. In addition, dissolved oxygen rapidly reoxidized the biogenic U(IV) to U(VI) and the reoxidation occurred as a sharp front moving through the porous media. To our knowledge, this in situ reoxidation experiment is the first such experiment to directly show through XANES spectroscopic analysis that bioreduced U(IV) can oxidize to U(VI) on the order of minutes when exposed to oxic conditions and the analysis is unique in that it tracked uranium speciation during oxidation over spatial and temporal scales. The fast rate at which U(IV) reoxidation occurred has important implications to the field-scale use of U(VI) biostimulation technologies and suggest that, at least for conditions similar to those used here, either active reducing conditions are maintained or the concentration of oxidants kept low in the reduced zone to avoid U(IV) reoxidation upon cessation of electron donor addition.

Acknowledgments

This research was funded by the Environmental Remediation Sciences Program (ERSP), Office of Biological and Environmental Research (OBER), U.S. Department of Energy (DOE) Grant No. DE-FG02-05ER63973. The *Geobacter metallireducens* strain used was provided by Derek Lovley (University of Massachusetts, Amherst, Mass.). X-ray absorption near edge structure (XANES) spectroscopy was performed at beamline X26A at the National Synchrotron Light Source (NSLS) at Brookhaven National Laboratory. X26A is supported by the DOE–Geosciences

(Contract No. DE-FG02-92ER14244), and DOE–Office of Biological and Environmental Research, ERSD. Use of NSLS was supported by DOE under Contract No. DE-AC02-98CH10886.

References

Abdelouas, A., Lutze, W., and Nuttall, H. E. (1999). "Oxidative dissolution of uraninite precipitated on Navajo sandstone." *J. Contam. Hydrol.*, 36(3–4), 353–375.

Anderson, R. T., et al. (2003). "Stimulating the *in situ* activity of *Geobacter* species to remove uranium from the groundwater of a uranium-contaminated aquifer." *Appl. Environ. Microbiol.*, 69(10), 5884–5891.

Ankudinov, A. L., Ravel, B., Rehr, J. J., and Conradson, S. D. (1998). "Real-space multiple-scattering calculation and interpretation of x-ray-absorption near-edge structure." *Phys. Rev. B*, 58(12), 7565–7576.

Boyanov, M. I., O'Loughlin, E. J., Roden, E. E., Fein, J. B., and Kemner, K. M. (2007). "Adsorption of Fe(II) and U(VI) to carboxyl-functionalized microspheres: The influence of speciation on uranyl reduction studied by titration and XAFS." *Geochim. Cosmochim. Acta*, 71(8), 1898–1912.

Brooks, S. C., et al. (2003). "Inhibition of bacterial U(VI) reduction by calcium." *Environ. Sci. Technol.*, 37(9), 1850–1858.

Chang, Y. J., et al. (2005). "Microbial incorporation of C-13-labeled acetate at the field scale: Detection of microbes responsible for reduction of U(VI)." *Environ. Sci. Technol.*, 39(23), 9039–9048.

Cheng, T., Barnett, M. O., Roden, E. E., and Zhuang, J. L. (2006). "Effects of solid-to-solution ratio on uranium(VI) adsorption and its implications." *Environ. Sci. Technol.*, 40(10), 3243–3247.

Duff, M. C., and Amrhein, C. (1996). "Uranium(VI) adsorption on goethite and soil in carbonate solutions." *Soil Sci. Soc. Am. J.*, 60(5), 1393–1400.

Elias, D. A., Senko, J. M., and Krumholz, L. R. (2003). "A procedure for quantitation of total oxidized uranium for bioremediation studies." *J. Offshore Mech. Arct. Eng.*, 53(3), 343–353.

Finneran, K. T., Housewright, M. E., and Lovley, D. R. (2002). "Multiple influences of nitrate on uranium solubility during bioremediation of uranium-contaminated subsurface sediments." *Environmental Microbiology*, 4(9), 510–516.

Fredrickson, J. K., Zachara, J. M., Kennedy, D. W., Duff, M. C., Gorby, Y. A., Li, S. M. W., and Krupka, K. M. (2000). "Reduction of U(VI) in goethite (alpha-FeOOH) suspensions by a dissimilatory metal-reducing bacterium." *Geochim. Cosmochim. Acta*, 64(18), 3085–3098.

Fredrickson, J. K., Zachara, J. M., Kennedy, D. W., Liu, C. X., Duff, M. C., Hunter, D. B., and Dohnalkova, A. (2002). "Influence of Mn oxides on the reduction of uranium(VI) by the metal-reducing bacterium *Shewanella putrefaciens*." *Geochim. Cosmochim. Acta*, 66(18), 3247–3262.

Freeze, R. A., and Cherry, J. A. (1979). *Groundwater*, Prentice-Hall, Englewood Cliffs, N.J.

Giammar, D. E., and Hering, J. G. (2001). "Time scales for sorption-desorption and surface precipitation of uranyl on goethite." *Environ. Sci. Technol.*, 35(16), 3332–3337.

Ginder-Vogel, M., Criddle, C. S., and Fendorf, S. (2006). "Thermodynamic constraints on the oxidation of biogenic UO_2 by Fe(III) (hydr) oxides." *Environ. Sci. Technol.*, 40(11), 3544–3550.

Gu, B. H., et al. (2005a). "Bioreduction of uranium in a contaminated soil column." *Environ. Sci. Technol.*, 39(13), 4841–4847.

Gu, B. H., Yan, H., Zhou, P., Watson, D. B., Park, M., and Istok, J. (2005b). "Natural humics impact uranium bioreduction and oxidation." *Environ. Sci. Technol.*, 39(14), 5268–5275.

Hsi, C. K. D., and Langmuir, D. (1985). "Adsorption of uranyl onto ferric oxyhydroxides: Application of surface complexation site-binding model." *Geochim. Cosmochim. Acta*, 49, 1931–1941.

Ilton, E. S., Heald, S. M., Smith, S. C., Elbert, D., and Liu, C. X. (2006). "Reduction of uranyl in the interlayer region of low iron micas under anoxic and aerobic conditions." *Environ. Sci. Technol.*, 40(16), 5003–5009.

Istok, J. D., Senko, J. M., Krumholz, L. R., Watson, D., Bogle, M. A., Peacock, A., Chang, Y. J., and White, D. C. (2004). "*In situ* bioreduction of technetium and uranium in a nitrate-contaminated aquifer." *Environ. Sci. Technol.*, 38(2), 468–475.

Jeon, B. H., Kelly, S. D., Kemner, K. M., Barnett, M. O., Burgos, W. D., Dempsey, B. A., and Roden, E. E. (2004). "Microbial reduction of U(VI) at the solid-water interface." *Environ. Sci. Technol.*, 38(21), 5649–5655.

Kelly, S. D., Kemner, K. M., Fein, J. B., Fowle, D. A., Boyanov, M. I., Bunker, B. A., and Yee, N. (2002). "X-ray absorption fine structure determination of pH-dependent U-bacterial cell wall interactions." *Geochim. Cosmochim. Acta*, 66(22), 3855–3871.

Komlos, J., and Jaffe, P. R. (2004). "Effect of iron bioavailability on dissolved hydrogen concentrations during microbial iron reduction." *Biodegradation*, 15(5), 315–325.

Lack, J. G., Chaudhuri, S. K., Kelly, S. D., Kemner, K. M., O'Connor, S. M., and Coates, J. D. (2002). "Immobilization of radionuclides and heavy metals through anaerobic bio-oxidation of Fe(II)." *Appl. Environ. Microbiol.*, 68(6), 2704–2710.

Langmuir, D. (1978). "Uranium solution-mineral equilibria at low-temperatures with applications to sedimentary ore-deposits." *Geochim. Cosmochim. Acta*, 42(6), 547–569.

Lovley, D. R., and Phillips, E. J. P. (1987). "Rapid assay for microbially reducible ferric iron in aquatic sediments." *Appl. Environ. Microbiol.*, 53(7), 1536–1540.

Lovley, D. R., and Phillips, E. J. P. (1988). "Novel mode of microbial energy-metabolism—Organic-carbon oxidation coupled to dissimilatory reduction of iron or manganese." *Appl. Environ. Microbiol.*, 54(6), 1472–1480.

Lovley, D. R., and Phillips, E. J. P. (1992). "Reduction of uranium by *Desulfovibrio-desulfuricans*." *Appl. Environ. Microbiol.*, 58(3), 850–856.

Michalsen, M. M., Goodman, B. A., Kelly, S. D., Kemner, K. M., McKinley, J. P., Stucki, J. W., and Istok, J. D. (2006). "Uranium and technetium bio-immobilization in intermediate-scale physical models of an in situ bio-barrier." *Environ. Sci. Technol.*, 40(22), 7048–7053.

Moon, H. S., Komlos, J., and Jaffe, P. R. (2007). "Uranium reoxidation in previously bioreduced sediment by dissolved oxygen and nitrate." *Environ. Sci. Technol.*, 41(13), 4587–4592.

Newville, M. (2001). "IFEFFIT: Interactive XAFS analysis and FEFF fitting." *J. Synchrotron Radiat.*, 8, 322–324.

Newville, M., Livins, P., Yacoby, Y., Rehr, J. J., and Stern, E. A. (1993). "Near-edge X-ray-absorption fine-structure of Pb—A comparison of theory and experiment." *Phys. Rev. B*, 47(21), 14126–14131.

Newville, M., Ravel, B., Haskel, D., Rehr, J. J., Stern, E. A., and Yacoby, Y. (1995). "Analysis of multiple-scattering XAFS data using theoretical standards." *Physica B*, 209(1–4), 154–156.

O'Loughlin, E. J., Kelly, S. D., Cook, R. E., Csencsits, R., and Kemner, K. M. (2003). "Reduction of uranium(VI) by mixed iron(II)/iron(III) hydroxide (green rust): Formation of UO_2 nanoparticles." *Environ. Sci. Technol.*, 37(4), 721–727.

Ortiz-Bernad, I., Anderson, R. T., Vrionis, H. A., and Lovley, D. R. (2004). "Resistence of solid-phase U(VI) to microbial reduction during in situ bioremediation of uranium-contaminated groundwater." *Appl. Environ. Microbiol.*, 70(12), 7558–7560.

Ravel, B., and Newville, M. (2005). "ATHENA, ARTEMIS, HEPHAESTUS: Data analysis for X-ray absorption spectroscopy using IFEFFIT." *J. Synchrotron Radiat.*, 12, 537–541.

Sandino, A., and Bruno, J. (1992). "The solubility of $(UO_2)_3(PO_4)_2 * 4H_2O(s)$ and the formation of U(VI) phosphate complexes—Their influence in uranium speciation in natural-waters." *Geochim. Cosmochim. Acta*, 56(12), 4135–4145.

Sani, R. K., Peyton, B. M., Dohnalkova, A., and Amonette, J. E. (2005). "Reoxidation of reduced uranium with iron(III) (hydr)oxides under sulfate-reducing conditions." *Environ. Sci. Technol.*, 39(7), 2059–2066.

Senko, J. M., Istok, J. D., Suflita, J. M., and Krumholz, L. R. (2002). "*In-situ* evidence for uranium immobilization and remobilization." *Environ. Sci. Technol.*, 36(7), 1491–1496.

Stern, E. A., and Heald, S. M. (1983). "Basic principles and applications of EXAFS." *Handbook of synchrotron radiation*, E. E. Koch, ed., North-Holland, Amsterdam, The Netherlands, 995–1014.

Stern, E. A., Newville, M., Ravel, B., Yacoby, Y., and Haskel, D. (1995). "The UWXAFS analysis package—Philosophy and details." *Physica B*, 209(1–4), 117–120.

Wan, J. M., et al. (2005). "Reoxidation of bioreduced uranium under reducing conditions." *Environ. Sci. Technol.*, 39(16), 6162–6169.

Wu, W. M., et al. (2006). "Pilot-scale *in situ* bioremediation of uranium in a highly contaminated aquifer: 2. Reduction of U(VI) and geochemical control of U(VI) bioavailability." *Environ. Sci. Technol.*, 40(12), 3986–3995.

Zheng, Z. P., Tokunaga, T. K., and Wan, J. M. (2003). "Influence of calcium carbonate on U(VI) sorption to soils." *Environ. Sci. Technol.*, 37(24), 5603–5608.

Zhou, P., and Gu, B. H. (2005). "Extraction of oxidized and reduced forms of uranium from contaminated soils: Effects of carbonate concentration and pH." *Environ. Sci. Technol.*, 39(12), 4435–4440.